Redox and catalytic behaviors of chromium oxide supported on zirconia

Jong Rack Sohn [a,*] and Sam Gon Ryu [b]

[a] *Department of Industrial Chemistry, Engineering College, Kyungpook National University, Daegu 702-701, Korea*
[b] *Agency for Defense Development, PO Box 35, Yuseong, Taejon 305-600, Korea*

Received 14 February 2001; accepted 5 April 2001

Chromium oxide supported on zirconia was prepared by dry impregnation of powdered $Zr(OH)_4$ with an aqueous solution of $(NH_4)_2CrO_4$ followed by calcining in air. Upon the addition of only a small amount of chromium oxide (1 wt% Cr) to ZrO_2, both the acidity and acid strength of the catalyst increased remarkably. The redox and catalytic behaviors of the samples were investigated through XPS and the reaction of cumene using a pulse technique. It was found that Cr^{6+} species existing on the surface of catalyst were responsible for the formation of strong acid sites and the catalytic activity for cracking of cumene. However, the Cr^{6+} species were easily reduced to Cr^{3+} species during the catalytic reaction of cumene and the reduced Cr^{3+} species were active for α-methylstyrene formation due to the dehydrogenation of cumene. The reduced Cr^{3+} species could be reoxidized by treatment with O_2 and subsequently the reoxidized catalyst exhibited catalytic activity for the cracking reaction of cumene.

KEY WORDS: chromium oxide; redox and catalytic behaviors; XPS; dehydrogenation of cumene; cracking of cumene

1. Introduction

Supported chromium oxide catalysts are being used for the polymerization, hydrogenation, and oxidation–reduction reactions between environmentally important molecules such as CO and NO [1–6]. Recently, many efforts have involved the characterization of these catalysts in an attempt to find the appropriate reaction mechanisms. Titrations to determine the oxidation state of the chromium used in conjunction with infrared and electron paramagnetic resonance spectroscopy have provided much information dealing with these questions. So far, however, they have been studied mainly on silica and alumina [7–10], and only a small amount of work was done for the ZrO_2 support [11–13].

Zirconia is an important material due to its interesting thermal and mechanical properties and so has been investigated as a support and catalyst in recent years. Different papers have been devoted to the study of ZrO_2 catalytic activity in important reactions such as methanol and hydrocarbon synthesis from CO and H_2 or CO_2 and H_2 [14–16] or alcohol dehydration [17–19]. Zirconia has been extensively used as a support for metals or incorporated in supports to stabilize them or make them more resistant to sintering [20–24]. ZrO_2 activity and selectivity highly depend on the methods of preparation and the treatment used. In particular, in previous papers from this laboratory, it has been shown that NiO–ZrO_2 and ZrO_2 modified with sulfate or tungstate ion are very active for acid-catalyzed reaction, even at room temperature [25–27]. The high catalytic activities in the above reaction were attributed to the enhanced acidic properties of the modified catalysts, which originate from the inductive effect of S=O and W=O bonds of the complex formed by the interaction of oxides with the sulfate or tungstate ion.

It is well known that the dispersion, the oxidation state, and the structural features of supported species may strongly depend on the support. Structure and physico-chemical properties of supported metal oxides are considered to be in different states compared with bulk metal oxides because of their interaction with supports. A previous paper described the surface characterization of chromium oxide supported on zirconia [28]. As an extension of our study on supported catalysts, in this work we deal with redox and catalytic behaviors of chromium oxide supported on zirconia. For this purpose, cumene was used as a test reactant.

2. Experimental

2.1. Catalysts

The precipitate of $Zr(OH)_4$ was obtained by adding aqueous ammonia slowly into an aqueous solution of zirconium oxychloride at room temperature with stirring until the pH of either liquor reached about 8. The precipitate thus obtained was washed thoroughly with distilled water until chloride ion was not detected, and was dried at room temperature for 12 h. The dried precipitate was ground to a powder smaller than 100 mesh.

Samples containing various contents of chromium were prepared by dry impregnation of powdered $Zr(OH)_4$ with aqueous solution of $(NH_4)_2CrO_4$ followed by calcining at high temperature for 1.5 h in air. This series of catalysts are

* To whom correspondence should be addressed.

1011-372X/01/0600-0105$19.50/0

denoted by their wt% of chromium and calcination temperature. For example, 1-CrO_x/ZrO_2-600 indicates the catalyst containing 1 wt% chromium calcined at 600 °C.

2.2. Procedure

X-ray photoelectron spectra were obtained with a VG Scientific model ESCALAB MK-11 spectrometer. Al Kα and Mg Kα were used as the excitation source, usually at 12 kV, 20 mA. The analysis chamber was 10^{-9} Torr or better and the spectra of samples, as fine powder, were analyzed. However, to examine the redox behavior of catalysts, some samples were pressed onto a plate, treated with H_2 and O_2 flowing at 10 ml/min for 6 min at 550 °C in a separate gas cell, and transferred into an analysis chamber without exposure to air. Binding energies were referenced to the C 1s level of the adventitious carbon at 285.0 eV.

The acid strength of the catalysts was measured qualitatively after pretreatments using a series of Hammett indicators [25–27]. The catalysts were pretreated in glass tubes by the same procedure as for the reactions. They were cooled to room temperature and filled with dry nitrogen. The color changes of a series of indicators were observed for each catalyst by the spot test under dry nitrogen. Chemisorption of ammonia was employed as a measure of acidity of the catalysts. The amount of chemisorption was obtained as an irreversible adsorption of ammonia [29,30]. The specific surface area was determined by applying the BET method to the adsorption nitrogen at −196 °C.

Catalytic activities for cumene reactions over CrO_x/ZrO_2 were measured in a pulse microreactor constructed of 1/4 inch stainless steel. For each experiment, 0.08 g of catalyst was loaded into a reactor. The reactor was packed with quartz chips that both positioned the catalyst sample near an external thermocouple and served as a preheating stage for the reactant gas. The catalyst samples were activated *in situ* by heating them under flowing He gas for 2 h at various temperatures. Pulses of 1 μl reactant were injected into a He gas stream which passed over 0.08 g catalyst at 20 ml/min. The cumene reactions were carried out at 350–600 °C. Reaction products were analyzed by gas chromatography equipped with a Bentone 34 on Chromosorb W column at 130 °C. Catalytic activity was represented as μmol of reacted cumene per g catalyst. Conversions for cumene reactions were taken as the average of the fourth to tenth pulse value.

3. Results and discussion

3.1. Surface area

The specific surface areas of samples calcined at 600 °C for 1.5 h are plotted as a function of chromium content in figure 1. The presence of chromium oxide strongly influences the surface area in comparison with the pure ZrO_2. Specific surface areas of CrO_x/ZrO_2 samples are much larger than that of pure ZrO_2 calcined at the same temperature,

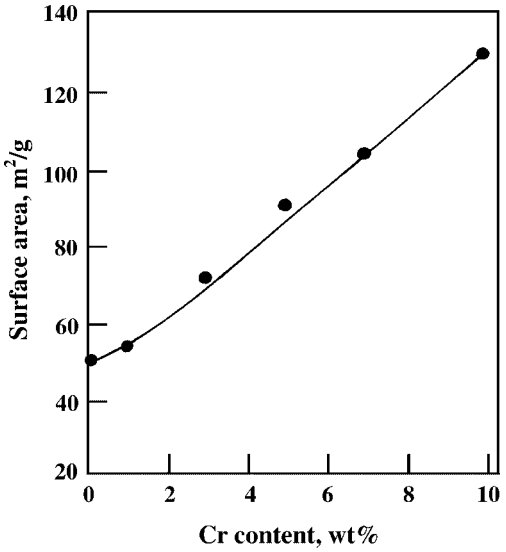

Figure 1. Variation of surface area of CrO_x/ZrO_2 calcined at 600 °C with chromium content.

showing that surface area increases gradually with increasing chromium content. It seems likely that the interaction between chromium oxide and ZrO_2 protects catalysts from sintering [28]. The dependence of antisintering effect on chromium oxide content is clear from figure 1. These results are correlated with the fact that the transition temperature of ZrO_2 from amorphouse to tetragonal phase increases with increasing chromium oxide content in DTA and XRD experiments reported previously [28].

3.2. Acidic properties

The acid strength of the catalysts was examined by a color change method, using a Hammett indicator in sulfuryl chloride [25–27]. Since it was very difficult to observe the color of indicators adsorbed on catalysts of high chromium oxide content, a low percentage of chromium content (0.1 wt%) was used in this experiment. The results are listed in table 1. In this table, + indicates that the color of the base form was changed to that of the conjugated acid form. ZrO_2 evacuated at 400 °C for 1 h has an acid strength $H_0 \leqslant 1.5$, while 0.1-CrO_x/ZrO_2 was estimated to have a $H_0 \leqslant -14.5$, indicating the formation of new acid sites stronger than those of single oxide components. The acid strength of 0.1-CrO_x/ZrO_2 oxidized with O_2 at 500 °C was also found to be $H_0 \leqslant -14.5$, while 0.1-CrO_x/ZrO_2 reduced with CO at 500 °C was estimated to have a $H_0 \leqslant -8.2$. Acids stronger than $H_0 \leqslant -11.93$, which corresponds to the acid strength of 100% H_2SO_4, are superacids [31]. Consequently, CrO_x/ZrO_2 catalysts except for the reduced sample would be solid superacids. The superacidic property is attributed to the double bond nature of the Cr=O in the complex formed by the interaction of ZrO_2 with chromate as

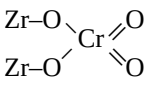

Table 1
Acid strengths of 0.1-CrO_x/ZrO_2 and ZrO_2.[a]

Hammett indicator	pK_a value of indicator	CrO_x/ZrO_2[b]	CrO_x/ZrO_2[c]	CrO_x/ZrO_2[d]	ZrO_2
Benzenazodiphenylamine	1.5	+	+	+	+
Dicinnamalacetone	−3.0	+	+	+	−
Benzalacetophenone	−5.6	+	+	+	−
Anthraquinone	−8.2	+	+	+	−
Nitrobenzene	−12.4	+	+	−	−
2,4-dinitrofluorobenzene	−14.5	+	+	−	−

[a] + indicates that the color of the base form was changed to that of the conjugated acid form.
[b] Calcined in air at 600 °C.
[c] Oxidized with O_2 at 500 °C.
[d] Reduced with CO at 500 °C.

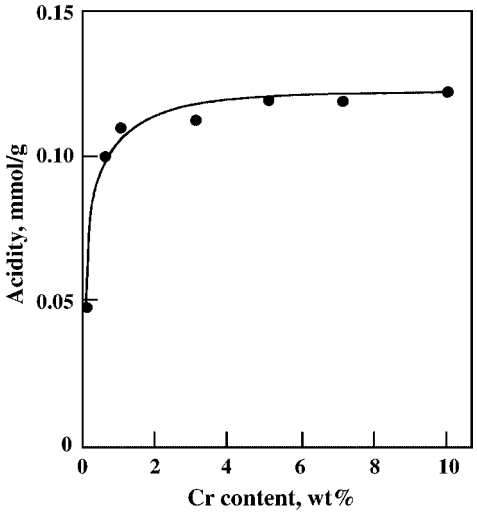

Figure 2. Acidity of CrO_x/ZrO_2 against chromium content.

in analogy with the case of ZrO_2 modified with sulfate ions [25–27].

The acidity of catalysts, as determined by the amount of NH_3 irreversibly adsorbed at 230 °C [28], is plotted as a function of the chromium content in figure 2. Although pure ZrO_2 shows the acidity of 0.05 meq/g, 1-CrO_x/ZrO_2 resulted in a remarkable increase in acidity (0.1 meq/g). As shown in figure 2, the acidity increases abruptly upon the addition of 1 wt% chromium to ZrO_2, and then the acidity increases very gently with increasing chromium oxide content. Many combinations of two oxides have been reported to generate acid sites on the surface [32]. The combination of ZrO_2 and CrO_x probably generates stronger acid sites and more acidity as compared with the separate components. A mechanism for the generation of acid sites by mixing two oxides has been proposed by Tanbe *et al.* [32]. They suggest that the acidity generation is caused by an excess of a negative or positive charge in a model structure of a binary oxide related to the coordination number of a positive element and a negative element.

3.3. XPS

The difficulty in the study of supported chromium oxide comes from the simultaneous presence of oxidation states.

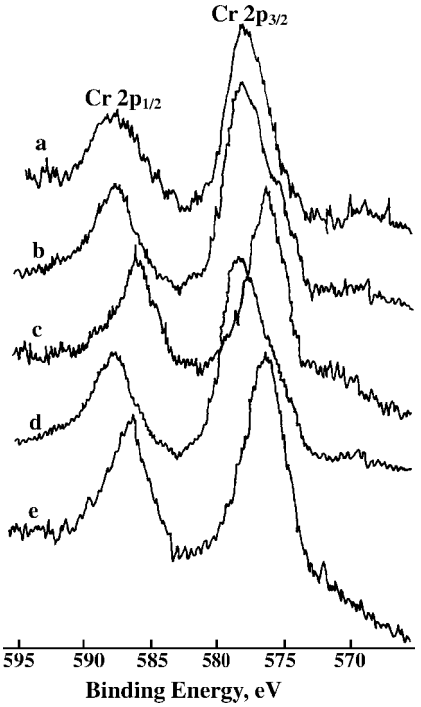

Figure 3. Cr 2p XPS of 3-CrO_x/ZrO_2 treated under various conditions: (a) uncalcined sample, (b) sample calcined at 600 °C, (c) after reduction of sample (b) with H_2 at 550 °C, (d) after reoxidation of sample (c) with O_2 at 550 °C, and (e) after reaction of sample (b) with cumene at 550 °C.

Figure 3 shows the Cr 2p spectra of 3-CrO_x/ZrO_2 treated under various conditions. The shape of peaks and binding energies of the 2p electron are different depending on the treatment conditions, indicating that the oxidation state of chromium varies with the treatment process.

To obtain further information on the oxidation state, the spectrum in the Cr $2p_{3/2}$ region was analyzed by appropriate curve fitting and the presence of two components was confirmed, as shown in figure 4. For the noncalcined and calcined samples, we have obtained a Cr $2p_{3/2}$ binding energy of 579.3 eV due to Cr(VI) and a binding energy of 576.7 eV identified as Cr(III). Cimino and co-workers have measured Cr 2p binding energies for a variety of different chromium compounds [33]. The corresponding Cr $2p_{3/2}$ binding energies for CrO_3 and Cr_2O_3 are 579.9 and 576.8 eV, respectively. The results of quantitative analysis for the chromium

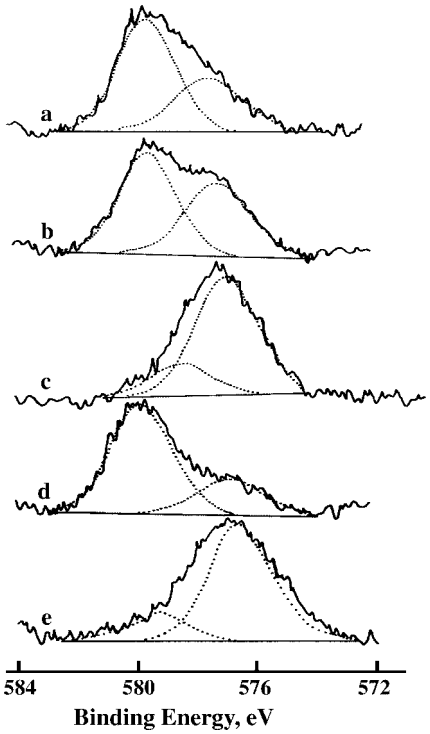

Figure 4. Cr $2p_{3/2}$ fitted XPS of 3-CrO_x/ZrO_2 treated under various conditions: (a) uncalcined sample, (b) sample calcined at 600 °C, (c) after reduction of sample (b) with H_2 at 550 °C, (d) after reoxidation of sample (c) with O_2 at 550 °C, and (e) after reaction of sample (b) with cumene at 450 °C.

Table 2
Percentage of chromium species from the area of the fitted bands in the Cr $2p_{3/2}$ XPS region.

Treatment condition	Cr^{6+}	Cr^{3+}
Uncalcined sample	65	35
Calcined air at 600 °C	54	46
After reduction with H_2 at 550 °C	22	78
After oxidation with O_2 at 550 °C	59	41
After reaction with cumene at 450 °C	20	80

oxidation state are listed in table 2. It is noted that the number of Cr(III) increases to some extent by the calcination at 600 °C.

However, Cr(VI) concentration of the sample calcined at 600 °C is quite large, being 54% of the total Cr concentration, indicating that the ZrO_2 support stabilizes supported chromium oxide. However, when sample (b) in figure 4 was treated with H_2 (10 ml/min) at 550 °C for 6 min, Cr(VI) species were easily reduced to Cr(III) species, as illustrated in figure 4(c) and table 2. Sample (c) was reoxidized with O_2 (10 ml/min) at 550 °C for 6 min and its XPS result is shown in figure 4(d). The Cr(VI)/Cr(III) ratio increased, which indicates that the reduction–oxidation process is reversible. For the cumene reaction a pulse-type microreactor, constructed of 1/4 inch stainless steel was used. Ten pulses of 1 μl of cumene were injected successively into a He gas stream which passed over 0.08 g of sample calcined at 550 °C at 15 ml/min. The reaction temperature was

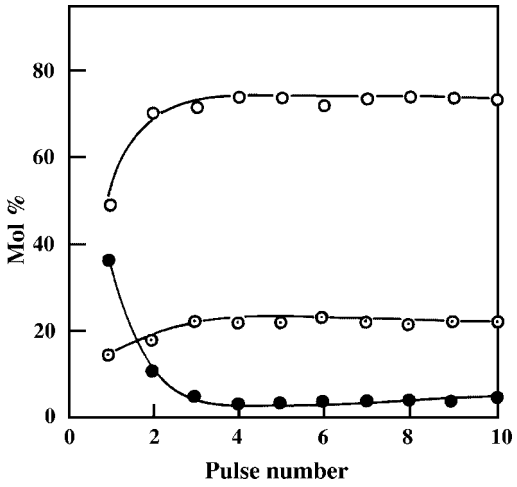

Figure 5. Variation of the amounts (mol%) of products and reactant after cumene reaction at 450 °C over 1-CrO_x/ZrO_2-600 with pulse number: (○) α-methylstyrene, (●) benzene, and (⊙) cumene.

450 °C. XPS of the catalyst after reaction is illustrated in figure 4(e), resulting in the increase of Cr(III) concentration.

3.4. Redox and catalytic behaviors

Chromium oxide catalysts exhibit different catalytic behavior depending on the oxidation state of chromium species supported on metal oxides [1–5]. We tested the cumene reaction at 450 °C over the chromium oxide–zirconia catalyst using a pulse technique so that the occurrence of two main catalytic reactions, cracking and dehydrogenation, was observed. Figure 5 shows the variations of the amount of products and reactant after cumene reaction over 1-CrO_x/ZrO_2-600 with pulse number. The products were identified to be α-methylstyrene due to the dehydrogenation reaction and identified to be propylene and benzene formed through the cracking reaction. As shown in figure 5, however, at the first pulse the cracking reaction occurred more predominantly than the dehydrogenation reaction, while from the second pulse the dehydrogenation reaction was enhanced remarkably and then from the fourth pulse the catalytic activity for the reaction was nearly constant.

It has been known that cracking of cumene takes place at medium acid sites of the catalysts [34,35], while the active site for the dehydrogenation of cumene is Cr^{3+} [36]. The predominant cracking reaction of cumene at the first pulse can be explained from the fact that the chromium oxide catalyst calcined at 600 °C has strong acid sites because chromium species bonded to zirconia surface are mainly present as chromate (Cr^{6+}). As described above, CrO_x/ZrO_2 calcined at 600 °C has an acid strength $H_0 \leqslant -14.5$ and the main presence of chromate (Cr^{6+}) for the calcined sample was demonstrated by XPS.

The remarkable enhancement of the dehydrogenation reaction and concomitant decrease of the cracking reaction for cumene from the second pulse is responsible for the reduction of chromium species from 6+ to 3+ during cumene reaction. Namely, it seems likely that hydrogen produced

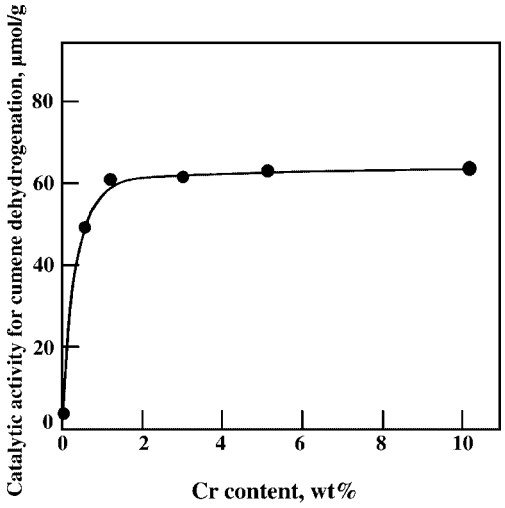

Figure 6. Catalytic activity of CrO_x/ZrO_2-600 for cumene dehydrogenation reaction as a function of chromium content.

through the dehydrogenation reaction of cumene reduces chromium species from 6+ to 3+. It was reported that supported chromium oxide is easily reduced by olefins or alcohol [9,37]. To obtain further information on oxidation state, the XPS in the Cr $2p_{3/2}$ region was analyzed. Ten pulses of 1 μl of cumene were injected successively into a He gas stream which passed over 0.08 g of sample calcined at 600 °C at 15 ml/min, where reaction temperature was 450 °C. The concentration of Cr^{3+} species for the sample calcined at 600 °C was 46%, while that of Cr^{3+} species after reaction with cumene was found to be 80% (figure 4(e) and table 2). From the above results it is clear that the active site for dehydrogenation of cumene is Cr^{3+} [36]. As listed in table 2, CrO_x/ZrO_2 reduced with CO has an acid strength $H_0 \leqslant -8.2$, indicating that the oxidation state of chromium species influences the acid strength and subsequent catalytic activities.

As shown in figure 5, CrO_x/ZrO_2 was catalytically active for the dehydrogenation reaction of cumene. The catalytic activity of 1-CrO_x/ZrO_2-600 for the dehydrogenation reaction as a function of reaction temperature was examined. The catalyst began to exhibit catalytic activity at 350 °C, giving a maximum at 450 °C. The samples calcined at other temperatures exhibited catalytic behavior similar to that calcined at 600 °C, also giving a maximum at 450 °C.

Catalytic activities of CrO_x/ZrO_2-600 for the dehydrogenation reaction are plotted as a function of chromium content in figure 6. Although pure ZrO_2 showed no catalytic activity, the addition of 1 wt% chromium to ZrO_2 resulted in a remarkable increase in activity, indicating that the element chromium is indispensable for the dehydrogenation reaction. As shown in figure 6, the activities increase abruptly upon the addition of chromium to ZrO_2 and then the activities are nearly constant. The patterns of catalytic activities in figure 6 are very similar to that of acidity in figure 2 except for pure ZrO_2. These results suggest that catalytic activity for dehydrogenation and acidity of CrO_x/ZrO_2 are correlated with the content of chromium oxide.

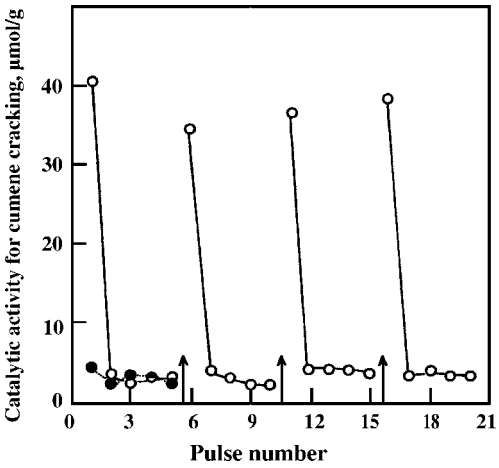

Figure 7. Cyclic behavior of catalytic property of 1-CrO_x/ZrO_2-600 for cumene cracking reaction, where (↑) indicates the interval of 20 ml O_2 injection and (•) indicates catalytic activity after reduction with 20 ml H_2 at 450 °C.

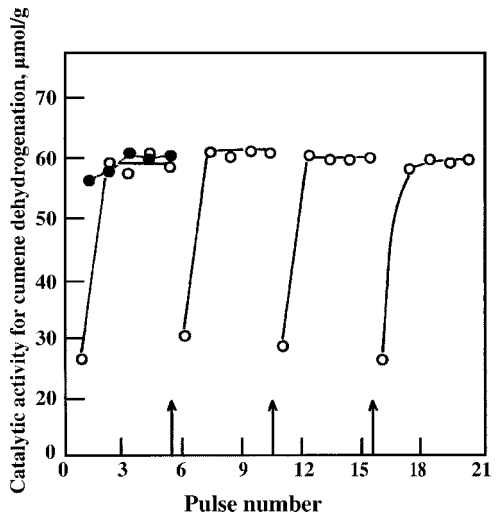

Figure 8. Cyclic behavior of catalytic property of 1-CrO_x/ZrO_2-600 for cumene dehydrogenation reaction, where (↑) indicates the interval of 20 ml O_2 injection and (•) indicates catalytic activity after reduction with 20 ml H_2 at 450 °C.

From the results of XPS described above and the analysis of products in figure 5 it is clear that Cr^{6+} species on the catalyst surface during cumene reaction are easily reduced to Cr^{3+} species. Cr^{3+} species reduced with H_2 were easily reoxidized to Cr^{6+} species by treatment with O_2, as shown in figure 4. Therefore, it is expected that the catalyst reduced with reactant cumene can be reoxidized by treating the reduced sample with O_2. To examine cyclic behavior of catalytic activity depending on the redox state of chromium species, a pulse microreactor was used and results are illustrated in figures 7 and 8.

3.5. Cyclic behavior of catalytic activity

Figure 7 shows cyclic behavior of catalytic activity for cumene cracking reaction at 450 °C. As shown in figure 7, at the first pulse cracking activity is very high, but from the

second pulse cracking activity drops suddenly because Cr^{6+} species are reduced to Cr^{3+} species during cumene reaction. Figure 7 also indicates the cracking activity of CrO_x/ZrO_2 after reduction with 20 ml H_2 at 450 °C, showing very low cracking activity. However, after the fifth pulse we treated the sample with 20 ml of O_2 at 500 °C and then at the sixth pulse the cracking activity was measured. The arrow in figure 7 indicates the interval of 20 ml O_2 injection. At the sixth pulse the cracking activity was completely recovered, but at the seventh pulse the cracking activity dropped suddenly due to the reduction of Cr^{6+} species, as it occurred at the second pulse. As shown in figure 7, catalytic behavior like this was repeated at every pulse after 20 ml O_2 injection, indicating that redox cycles of chromium species are reversible. In view of the XPS results, acid strength measurement, and the above cyclic behavior of cracking activity it is concluded that the catalyst having Cr^{6+} species is responsible for the cracking reaction of cumene.

Figure 8 shows cyclic behavior of catalytic activity for the dehydrogenation reaction of cumene at 450 °C. At the first pulse dehydrogenation activity is very low, but from the second pulse activity increases steeply because Cr^{3+} species formed from Cr^{6+} species by the reduction by H_2 produced during cumene reaction. Figure 8 also shows the dehydrogenation activity of CrO_x/ZrO_2 after reduction with 20 ml H_2 at 450 °C, giving very high activity. However, after the fifth pulse we oxidized the catalyst with 20 ml of O_2 as done in figure 7 and then at the sixth pulse dehydrogenation activity was estimated. The arrow in figure 8 indicates the interval of 20 ml O_2 injection. At the sixth pulse dehydrogenation activity dropped suddenly, but at the seventh pulse activity was nearly recovered due to the reduction of Cr^{6+} species, as it occurred at the second pulse. As shown in figure 8, catalytic behavior like this was repeated at every pulse after 20 ml O_2 injection, indicating the reversible and cyclic redox behavior of CrO_x/ZrO_2. From these results and XPS results, it seems likely that the active sites for the dehydrogenation reaction of cumene are Cr^{3+} species.

4. Conclusions

The presence of chromium oxide strongly influences the surface area in comparison with the pure ZrO_2 because the interaction between chromium oxide and ZrO_2 protects the catalyst from sintering. As a consequence the surface area of CrO_x/ZrO_2 increased gradually with increasing chromium oxide content. Upon the addition of only a small amount of chromium oxide to ZrO_2, both the activity and acid strength of the catalyst increased remarkably.

The redox and catalytic behaviors of CrO_x/ZrO_2 were investigated by using XPS and reacting cumene as a test reactant using a pulse technique. Cr^{6+} species existing on the surface of the catalyst were responsible for the formation of strong acid sites and the activity for cracking of cumene, while Cr^{3+} species were responsible for the activity for cumene dehydrogenation. However, the Cr^{6+} species were easily reduced to Cr^{3+} species during the catalytic reaction of cumene and the reduced Cr^{3+} species were also easily reoxidized by treating with O_2. Cyclic redox and catalytic behaviors of CrO_x/ZrO_2 were reversible.

References

[1] S. Wang, K. Murata, T. Hayakawa, S. Hamakawa and K. Suzuki, Appl. Catal. A 196 (2000) 1.
[2] D.L. Myers and J.H. Lunsford, J. Catal. 99 (1986) 140.
[3] D.W. Flick and M.C. Huff, Appl. Catal. A 187 (1999) 13.
[4] M.M.R. Feijen Jeurissen, J.J. Jorna, B.E. Nieuwenhuys, G. Sinquin, C. Petit and J.P. Hindermann, Catal. Today 54 (1999) 65.
[5] K. Köhler, J. Engweiler, H. Viebrock and A. Baiker, Langmuir 11 (1995) 3423.
[6] B.M. Weckhuysen, I.E. Wachs and R.A. Schoonheydt, Chem. Rev. 96 (1996) 3327.
[7] M.P. McDaniel, Adv. Catal. 33 (1985) 47.
[8] G. Ghiotti, E. Garrone and A. Zecchina, J. Mol. Catal. 46 (1988) 61.
[9] W. Hill and G. Öhlmann, J. Catal. 123 (1990) 147.
[10] H.G. El-Shobaky, A.M. Ghozza, G.A. El-Shobaky and G.M. Mohamed, Colloids Surf. 152 (1999) 315.
[11] A. Cimino, D. Cordischi, S. De Rossi, G. Ferraris, D. Gazzoli, V. Indovina, G. Minelli, M. Occhiuzzi and M. Valigi, J. Catal. 127 (1991) 744, 761, 777.
[12] G. Stenanić, S. Popović and S. Musić, Mater. Lett. 36 (1998) 240.
[13] M. Hino and K. Arata, J. Chem. Soc. Chem. Commun. 1355 (1987).
[14] I.A. Fisher and A.T. Bell, J. Catal. 178 (1998) 153.
[15] C. Su, J. Li, D. He, Z. Cheng and Q. Zhu, Appl. Catal. A 202 (2000) 81.
[16] T. Maehashi, K. Maruya, K. Domen, K. Aika and T. Onishi, Chem. Lett. 747 (1984).
[17] G. Larsen, E. Lotero, L. Petkovic and D.S. Shobe, J. Catal. 169 (1997) 169.
[18] R.A. Keogh, R. Srinivasan and B.H. Davis, J. Catal. 151 (1995) 292.
[19] J.R. Sohn and E.H. Park, J. Ind. Eng. Chem. 6 (2000) 297.
[20] J.R. Gonzalez-Velasco, M.A. Gutierrez-Ortiz, J.A. Gonzalez-Marcos, P. Pranda and P. Steltenpohl, J. Catal. 187 (1999) 24.
[21] P. Pranda and P. Steltenpohl, J. Catal. 187 (1999) 24.
[22] R. Burch and P.K. Loader, Appl. Catal. 143 (1996) 317.
[23] R. Szymanski, H. Charcosset, P. Gallezot, J. Massardier and L. Tournayan, J. Catal. 97 (1986) 366.
[24] M.E.S. Hengarty, A.M. O'Connor and J.R.H. Ross, Catal. Today 42 (1998) 225.
[25] J.R. Sohn and H.J. Kim, J. Catal. 101 (1986) 428.
[26] J.R. Sohn and D.C. Shin, J. Catal. 160 (1996) 314.
[27] J.R. Sohn and H.W. Kim, J. Mol. Catal. 52 (1989) 361.
[28] J.R. Sohn and S.G. Ryu, Langmuir 9 (1993) 126.
[29] J.R. Sohn, S.G. Cho, Y.I. Pae and S. Hayashi, J. Catal. 159 (1996) 170.
[30] J.R. Sohn and H.J. Jang, J. Mol. Catal. 64 (1991) 349.
[31] G.A. Olah, G.K.S. Prakash and J. Sommer, Science 206 (1979) 13.
[32] K. Tanabe, M. Misono, Y. Ono and H. Hattori, *New Soid Acid and Bases* (Kodansa, Tokyo, 1989) ch. 3, p. 108.
[33] A. Cimino, B.A. DeAngelis, A. Luchetti and G. Minelli, J. Catal. 45 (1976) 316.
[34] S.J. Decanio, J.R. Sohn, P.O. Fritz and J.H. Lunsford, J. Catal. 101 (1986) 132.
[35] J.R. Sohn, S.J. Decanio, P.O. Fritz and J.H. Lunsford, J. Phys. Chem. 90 (1986) 4847.
[36] W. Grunert, W. Saffert, R. Feldhaus and K. Anders, J. Catal. 99 (1986) 149.
[37] M.B. Leonard and W.L. Carrick, J. Org. Chem. 33 (1968) 616.